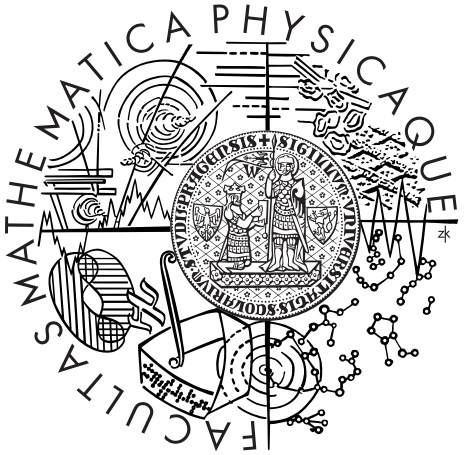
Charles University in Prague
Faculty of Mathematics and Physics

BACHELOR THESIS



Marie Michalová

Mathematical modeling of blood flows

Mathematical Institute, Charles University

Supervisor of the bachelor thesis: RNDr. Jaroslav Hron, Ph.D.
Study programme: Mathematics
Specialization: General Mathematics

Prague 2011

I would like to thank everybody who helped me with this work and the final language corrections, to everybody who was patient with me during the difficult times of creating this work and especially I would like to thank to my supervisor RNDr. Jaroslav Hron, Ph.D.

I declare that I carried out this bachelor thesis independently, and only with the cited sources, literature and other professional sources.

I understand that my work relates to the rights and obligations under the Act No.121/2000 Coll., the Copyright Act, as amended in particular the fact that the Charles University in Prague has the right to conclude a license agreement on the use of this work as a school work pursuant to Section 60 paragraph 1 of the Copyright Act.

In Prague, 25th of May 2011 Marie Michalová

Název práce: Matematické modelování proudění krve

Autor: Marie Michalová

Katedra: Matematický ústav UK

Vedoucí bakalářské práce: RNDr. Jaroslav Hron, Ph.D., MUUK

Abstrakt: Na začátku práce zmiňujeme některé důležité vlastnosti krve, její chování a vlastnosti jejích částí. V další části práce se zabýváme ustáleným dvoudimenzionálním Poisseuilleovým prouděním mezi dvěma rovnoběžnými deskami. Ukazujeme analytické výsledky pro Newtonův a mocninný model viskozity. Podle pozorování Fahraeus-Lindquistova efektu se kombinacemi výše zmíněných modelů snažíme aproximovat model dvou tekutin. V poslední části zkoumáme pulzační Poisseuilleovo proudění, pro které se zabýváme numerickými řešeními, a u nejjednoduššího Newtonova modelu i analytickým řešením, pro dané hodnoty tlaku a viskozity. Nakonec předkládáme náš nejlepší model, kde posouváme gradient tlaku a tím se více přiblížíme k reálným pozorováním.

Klíčová slova: krev, Poisseuillovo proudění, model dvou tekutin, pulsační proudění

Title: Mathematical modeling of blood flows

Author: Marie Michalová

Department: Mathematical Institute of Charles University

Supervisor: RNDr. Jaroslav Hron, Ph.D., MUUK

Abstract: At first we point out some important properties and behaviour of blood and blood particles. In the next part we approximate steady two-dimensional Poisseiulle flow between two parallel plates. We show analytical solutions for Newtonian and power-law models. According to observations of Fahraeus-Lindquist effect we show two-layer models combining previously mentioned models. In the last section we model pulsatile Poisseuille flow and we show analytical and numerical results for some pressure and viscosity values. In the end we show our best model, where we shift pressure gradient and get closer to the real blood flow characteristics.

Keywords: blood, Poisseuille flow, two-fluid model, pulsatile flow

Contents

Introduction **2**

1 Properties of blood **3**
1.1 Plasma . . . 3
1.2 Erythrocytes . . . 3
1.3 Leukocytes . . . 3
1.4 Thrombocytes . . . 4
1.5 Behaviour of Blood . . . 4
1.6 Description of blood flow . . . 5
1.7 Blood models in this thesis . . . 6

2 Derivation of the basic equations **7**
2.1 Dimensionless form of the equations . . . 8

3 Poisseuille Flow **9**
3.1 Approximating blood as one fluid . . . 9
3.1.1 Newtonian Fluid . . . 9
3.1.2 Power-law Model . . . 10
3.1.3 Application of the Boundary Conditions . . . 11
3.1.4 Different choice of constants . . . 12
3.1.5 Determination of pressure according to flow rate . . . 12
3.2 Two Fluid Models . . . 13
3.2.1 Two fluid Constant Viscosity . . . 14
3.2.2 Two fluid Power-law Model . . . 15
3.2.3 Two fluid combined Model . . . 15
3.2.4 Comparison of the models . . . 16

4 Pulsatile Flow **18**
4.1 Derivation of the basic equation . . . 18
4.2 Analytical solution for oscillating pressure . . . 18
4.3 Numerical solution for oscillating pressure . . . 20
4.3.1 One-fluid models . . . 21
4.3.2 Two-fluid models . . . 23
4.4 Numerical solution for shifted pressure . . . 25

Epilogue **26**

Bibliography **27**

Attachments **28**

Introduction

Blood is the most important fluid in our bodies. It forms approximately 8% of the body weight, transports oxygen and nutrients into the body tissues and takes away the metabolic waste products.

The first attempts to understand the mechanism of blood flow started hundreds of years ago in the times of da Vinci and Descartes. The biggest obstacle was that blood in blood vessels does not behave like an ideal fluid in rigid tubes, as it was assumed at first. However, with a correct interpretation the mechanical principles can give us some basic ideas about the blood behaviour.

In this work we model the Fahraeus-Lindquist effect. It is observed that the flowing blood is divided into two layers, the outer layers of plasma and the central area consisting mainly of blood particles. We show two basic models: Newtonian model and power-law model to capture the non-Newtonian behaviour of blood. We start with one-fluid and two-fluid models for steady flow, we show their analytical solutions and comparison after fitting them to the same flow rate.

In the second part of our work we try to approximate the pulsatile flow. As we get to non-linear partial differential equations we need to use some approximating algorithms and we show the numerical results. In the end we get to the best model, which is a two-fluid model with shifted pressure gradient. This is the closest one to the actual blood flow because it includes oscillating flow regime, non-Newtonian behaviour with shear dependent viscosity and Fahraeus-Lindquist effect captured by the two-fluid model approximation.

1. Properties of blood

Understanding the blood flow properties is very useful for example in surgery. Surgeons are provided with new materials, technologies and substitutions for human organs, which are very helpful on one hand but can for example cause formation of blood clots on the other hand. Therefore it is necessary to perceive the risks of using these materials and minimize them.

Blood is a suspension of blood particles in a water-like liquid. The liquid is called plasma and the dispersed components are represented by deformable corpuscular particles like erythrocytes, leukocytes and platelets.

We will now show an outline of the most important properties of blood particles, for detailed information see [7].

1.1 Plasma

Plasma forms about 55% of the blood volume. It is a suspension of proteins (e.g. albumin, globulin, fibrinogen) and an aqueous solution of inorganic and organic salts. When not moving, plasma loses its liquidity and tends to coagulate.

1.2 Erythrocytes

The red blood corpuscles are called erythrocytes and are numerically the most important components of blood. They form between 93% and 97% of the overall number of blood corpuscules. Each erythrocyte forms a disk, whose surface is made from a thin membrane and the interior is filled with a solution of haemoglobin. Because of the liquid content, erythrocytes are very deformable, may change their shape under the effects of shear stress from circular disc into elongated bodies and therefore may also pass through very small capillaries.

Because of their dimension, erythrocytes are considered the principal reason for the non-Newtonian behaviour of blood. It is the formation and decay of their aggregates that influences the blood viscosity.

The average size of erythrocytes is $7.5\mu m$, so we will be considering flow in arterioles of diameter about $0.5mm$ ($500\mu m$), which is the diameter of a small muscular arterie. For smaller diameters our models would not be valid and we would not be able to describe blood as a homogeneous fluid, we would have to consider each single corpuscle and its behaviour.

1.3 Leukocytes

The most important representatives of these white blood corpuscles are granulocytes and lymphocytes, they form up to 95% of all the leukocytes. Their size is between $7 - 12\mu m$ and they are responsible for protecting the body against infections and parasites.

Because they incline to agglomerate under ordinary physiological conditions, granulocytes are important also from the standpoint of biomechanics. When such agglomeration is formed, it adheres to the blood-vessels walls and thus increases

the resistance to flow and retards the blood flow. But for purposes of our work, we will be neglecting these situations.

1.4 Thrombocytes

Thrombocytes, also called blood platelets, are small granular particles and their number is relatively small compared to the number of erythrocytes - approximately 5%. Also their size is between $2 - 3\mu m$, which is a third of the diameter of erythrocytes. This means they do not directly influence the rheological properties of blood. However, they are very important in the process of wound healing and generally blood coagulation and therefore cannot be omitted.

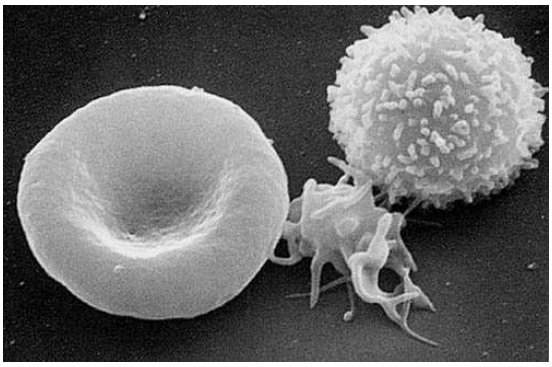


Figure 1.1: A scanning electron microscope image from blood particles, from left to right one can see an erythrocyte, thrombocyte and leukocyte. Taken from [9].

1.5 Behaviour of Blood

According to its structure, blood represents a non-Newtonian fluid and shows interesting properties. For example in arteries with small inner diameter the Fahraeus-Lindquist effect can be observed. This means a lower apparent viscosity in thinner tubes, which is usually being explained by higher concentration of blood corpuscles in the central region of the tube, while the region near the walls is almost particle-free and shows the features of Newtonian fluid.

One of such measurements was conducted in [4] with the laser-Doppler method. To obtain better results, they replaced the red blood cells by red cell ghosts, which do not absorb so much light and hence do not corrupt the experiment.

At first they tested how the platelets behave. In the absence of red cell ghosts they demonstrated a distribution of rigid particles in flow, which is called 'tubular pinch'. This means that the maximal platelet concentration was found at the position of $0.6R$, where R is the vessel radius, in the center of the tube the concentration was lower and was zero by the walls.

The concentration distribution of the red cell ghosts was similar to the distribution of deformable particles, the concentration was high at the axis of the tube and steadily decreased to zero toward the wall. This caused that the local

hematocrit at the axis of the tube was higher than the average tube hematocrit[1] while the hematocrit at the walls was under the average.

The distribution of the platelets changed significantly in the presence of ghosts. The particles migrated from the position of $0.6R$ to the walls and at the axis of the tube there remained almost no platelets. Such high platelets concentration at the wall might be the reason for different blood behaviour than was expected.

For more details concerning description of blood see [1], [7], [3] or [8].

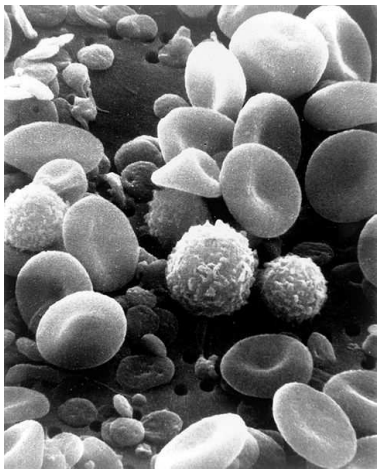


Figure 1.2: Erythrocytes, leukocytes and other blood platelets as can be found in normal human blood. Source [6].

1.6 Description of blood flow

For fluid characterization, we usually use the shear stress vs. shear rate curve. This is a graphical representation of experimental measurements which let us indirectly measure the fluid's viscosity.

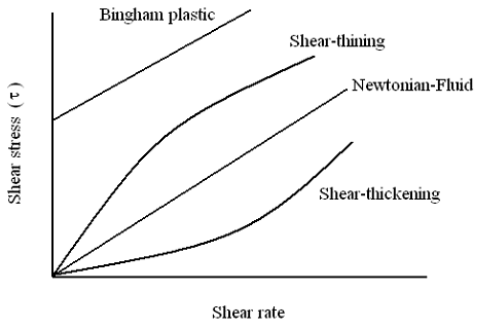


Figure 1.3: Dependence of shear stress on shear rate for different typs of fluids. Source [6].

[1]Hematocrit is defined as the ratio of the volume of the corpuscular components of blood to the volume of plasma.

Different types of fluids have different shapes of the shear stress-rate curves, see figure 1.3. Blood, for example, represents a shear-thinning, so called pseudo-plastic, fluid. This means that its viscosity is time independent, but decreases with increasing shear rate.

For measuring blood viscosity there are many types of viscometers. The most common is probably the Cone and Plate viscometer. It uses a cone with a very shallow angle and a plate, the shear rate is constant for the plate and the shear stress is measured at the cone (or vice versa; there are more types of these viscometers).

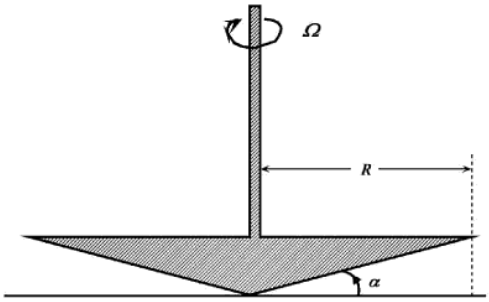


Figure 1.4: The schematic picture of Cone and Plate viscometer.

Other flow characteristic is the Reynolds number. It is a dimensionless number that gives a measure of the ratio of inertial forces to viscous forces and relates to both the flowing body and the medium surrounding it. It is used to determine similarities between different experimental cases and to distinguish laminar flow ($Re < 2300$) from turbulent flow ($Re > 4000$). Some typical values for blood flow in the human body are following:

blood flow in brain: Re $\approx 10^2$
blood flow in aorta: Re $\approx 10^3$

1.7 Blood models in this thesis

When talking about fluid modeling, we mean approximating some of the fluids' characteristic. Usually we try to describe its viscosity. In this thesis we will be using two basic models, Newtonian and Power-law, and we will be also considering their combinations in two-fluid models.

The assumption of Newtonian behaviour of blood is acceptable only for high shear rates of flow in large arteries. On the other hand Newtonian model is quite suitable for approximating plasma.

Power-law model is more suitable because it describes viscosity changes with shear rate. It can be also easily extended to Casson model, which is probably the best representative for human blood and is usually used in current literature, see [8]. It holds satisfactorily for blood in vessels of diameter between $130 - 1300\mu m$, which is the diameter of an average artery.

2. Derivation of the basic equations

The Navier-Stokes equations are named after Claude-Luis Navier, a French engineer and physicist who specialized in mechanics, and George Gabriel Stokes, an English mathematician and physicist. These equations were derived from the principles of mass, momentum and energy conservation for continuum mechanics and model the fluid motion. They are very useful because they can be applied to many problems from water flow in a tube to air flow around a wing.

The three general equations are following:

$$\frac{\partial(\rho \boldsymbol{v})}{\partial t} + \operatorname{div}(\rho \boldsymbol{v} \otimes \boldsymbol{v}) = \rho \boldsymbol{f} - \operatorname{div} \mathbb{T}, \tag{2.1}$$

$$\frac{\partial \rho}{\partial t} + \operatorname{div}(\rho \boldsymbol{v}) = 0, \tag{2.2}$$

$$\frac{\partial E}{\partial t} + \operatorname{div}(E\boldsymbol{v}) = \rho \boldsymbol{f} \cdot \boldsymbol{v} + \operatorname{div}(\mathbb{T}\boldsymbol{v}) + \rho r - \operatorname{div} \boldsymbol{q}, \tag{2.3}$$

where $\rho(t,x)$ is density of the fluid, $\boldsymbol{v}(t,x)$ is the velocity field, $\mathbb{T}$ is the stress tensor, $\boldsymbol{f}$ stands for other body forces (e.g. gravitation), E is the total energy, r is the density of heat sources and $\boldsymbol{q}$ is the heat flux.

Equation (2.1) was derived from the law of momentum conservation, equation (2.2) comes from the law of mass conservation and is called continuity equation and the last one, equation (2.3), was derived from energy conservation law.

For purposes of this work we will suppose following simplifications:
(a) the flow is two-dimensional,
(b) the flow is homogeneous, i.e. $\nabla \rho = 0$,
(c) we will neglect the body forces, i.e. $\boldsymbol{f} \equiv 0$,
(d) the flow is incompressible, i.e. $\frac{d\rho}{dt} = 0$
(e) the flow is isothermal.

Taking the equations 2.1, 2.2 and 2.3 stated above and simplifying them according to the statements (a) - (e), we get

$$\operatorname{div} \boldsymbol{v} = 0 \tag{2.4}$$

and

$$\rho \frac{\partial \boldsymbol{v}}{\partial t} + \rho \operatorname{div}(\boldsymbol{v} \otimes \boldsymbol{v}) = \operatorname{div} \mathbb{T} \tag{2.5}$$

where the functions $\boldsymbol{v}$ and $\mathbb{T}$ are only x_1, x_2 and time t dependent and ρ is the constant viscosity of the fluid.

Suppose the stress tensor in following form

$$\mathbb{T} = -p\mathbb{I} + 2\mu\mathbb{D},$$

where p is the pressure, $\mu > 0$ is the viscosity coefficient and $\mathbb{D} = (d_{ij})_{i,j=1}^{3}$ with $d_{ij} = \frac{1}{2}\left(\frac{\partial v_i}{\partial x_j} + \frac{\partial v_j}{\partial x_i}\right)$ is the rate of deformation tensor. Using this form of stress tensor, we can further simplify the equation (2.5) and get

$$\rho \frac{\partial \boldsymbol{v}}{\partial t} + \rho \operatorname{div}(\boldsymbol{v} \otimes \boldsymbol{v}) = -\nabla p + \operatorname{div}(2\mu\mathbb{D}). \tag{2.6}$$

2.1 Dimensionless form of the equations

In practice it is useful to normalize all the variables and take a look on the dimensionless solution, so that we don't have to change our results for different size of vessels.

Let us define typical length L (e.g. distance of two parallel plates) and typical velocity V (e.g. mainstream velocity). Now we define the dimensionless position

$$\bar{x} = \frac{x}{L},$$

dimensionless time

$$\bar{t} = \frac{tV}{L},$$

dimensionless velocity

$$\bar{\boldsymbol{v}}\left(\bar{t}, \bar{x}\right) = \frac{1}{V}\boldsymbol{v}\left(t, x\right)$$

and dimensionless pressure

$$\bar{p}\left(\bar{t}, \bar{x}\right) = \frac{1}{\rho V^2} p\left(t, x\right).$$

This yields

$$\frac{\partial}{\partial \bar{x}} = \frac{1}{L}\frac{\partial}{\partial \bar{x}},$$
$$\frac{\partial}{\partial \bar{t}} = \frac{L}{V}\frac{\partial}{\partial t}$$

and we can simplify the equations (2.6) and (2.4). On dropping the bars we get Navier-Stokes equations in following form

$$\operatorname{div} v = 0, \tag{2.7}$$

$$\frac{\partial \boldsymbol{v}}{\partial t} + \operatorname{div}\left(\boldsymbol{v} \otimes \boldsymbol{v}\right) = -\nabla p + 2 \operatorname{div}\left(\frac{1}{Re}\mathbb{D}\right), \tag{2.8}$$

where $Re = \frac{\rho}{\mu} LV$ is the Reynolds number.

3. Poisseuille Flow

At first we will solve the steady symmetric Poiseuille flow between two parallel plates. It is a simplified problem where we consider a constant pressure gradient $\nabla p = (P, 0)$[1] and a special form of velocity $\boldsymbol{v}(t, x_1, x_2) = (v_1(x_2), 0)$, see figure 3.1. This means that the velocity only depends on the distance from the plates and lets us simplify the rate of deformation tensor $\mathbb{D}$ into following form

$$\mathbb{D} = \begin{pmatrix} 0 & \frac{1}{2}\frac{\partial v_1}{\partial x_2} \\ \frac{1}{2}\frac{\partial v_1}{\partial x_2} & 0 \end{pmatrix}. \tag{3.1}$$

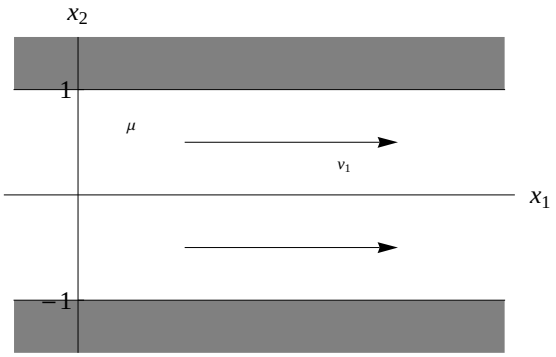


Figure 3.1: Poisseuille flow

3.1 Approximating blood as one fluid

Considering the Poisseuille flow, the equation (2.8) simplifies to

$$\nabla p = 2 \operatorname{div}(\mu \mathbb{D}). \tag{3.2}$$

We will consider two basic models, Newtonian model for constant viscosity and Power-law model, where the viscosity changes with shear rate.

3.1.1 Newtonian Fluid

Considering constant viscosity, equations (3.2) simplify to following form

$$\frac{\partial p}{\partial x_1} = \mu \frac{\partial^2 v_1}{\partial x_2^2} \tag{3.3}$$

$$\frac{\partial p}{\partial x_2} = 0, \tag{3.4}$$

where μ is the fluid's viscosity. These are two ordinary differential equations. The second equation only tells us that the pressure has to be x_2 independent but we are already considering constant pressure gradient. However, the first equation is

[1] For purposes of this work we will sometimes use the name 'pressure gradient' for P.

an equation with separated variables and can be solved by two integrations. The general solution is

$$v_1(x_2) = \frac{P}{2\mu}x_2^2 + C_1 x_2 + C_2, \tag{3.5}$$

where P stands for $\frac{\partial p}{\partial x_1} = const$ and C_1, C_2 are integration constants which will be specified later by applying the boundary conditions.

3.1.2 Power-law Model

Assuming Poisseuille flow and power-law model for viscosity which can be expressed as

$$\mu = \mu_0(\epsilon + |\mathbb{D}|^2)^{\frac{\alpha}{2}}, \tag{3.6}$$

where $\alpha \in (-1, 0)$, $\epsilon > 0$ and $|\mathbb{D}|^2 = \sum_{i,j=1}^{2} d_{ij}^2$ is the Frobenius norm of matrix. On substituting (3.6) into (3.2) we can rewrite equation (2.8) into

$$\nabla p = \mu_0 \operatorname{div} \begin{pmatrix} 0 & (\epsilon + |\mathbb{D}|^2)^{\frac{\alpha}{2}} \frac{\partial v_1}{\partial x_2} \\ (\epsilon + |\mathbb{D}|^2)^{\frac{\alpha}{2}} \frac{\partial v_1}{\partial x_2} & 0 \end{pmatrix}.$$

This gives us two equations

$$\frac{\partial p}{\partial x_1} = \mu_0 \frac{\partial}{\partial x_2} \left[\left(\epsilon + |\mathbb{D}|^2\right)^{\frac{\alpha}{2}} \frac{\partial v_1}{\partial x_2} \right] \tag{3.7}$$

and

$$\frac{\partial p}{\partial x_2} = 0.$$

The second equation again tells us that the pressure is x_2 independent. However, by integrating the first equation we get

$$\frac{P}{\mu_0}x_2 + D_1 = \left(\epsilon + \frac{1}{2}\left(\frac{\partial v_1}{\partial x_2}\right)^2\right)^{\frac{\alpha}{2}} \frac{\partial v_1}{\partial x_2}$$

where P stands for $\frac{\partial p}{\partial x_1}$. In order to get the analytical solution of this equation, we will assume $\epsilon = 0$. This assumption leads to

$$2^{\frac{\alpha}{2}}\left(\frac{P}{\mu_0}x_2 + D_1\right) = \left|\frac{\partial v_1}{\partial x_2}\right|^{\alpha} \frac{\partial v_1}{\partial x_2}, \quad \alpha \in (-1, 0)$$

but restricts the condition for velocity. When considering blood, α is negative, and therefore we need to ensure that $\frac{\partial v_1}{\partial x_2} \neq 0$. However, for the two-dimensional Navier-Stokes equations we know that the solution is unique, so if we find a solution we will not need to get back to this restriction. From symmetry and symmetric boundary conditions, we can assume $\frac{\partial v_1}{\partial x_2} < 0$. This yields

$$-2^{\frac{\alpha}{2}}\left(\frac{P}{\mu_0}x_2 + D_1\right) = \left(-\frac{\partial v_1}{\partial x_2}\right)^{\alpha+1}. \tag{3.8}$$

We see that before continuing we have to ensure that the term on the left side of equation (3.8) is not negative. This holds for $x_2 > -\frac{\mu_0}{P} D_1$ and we get

$$2^{\frac{\alpha}{2(\alpha+1)}} \int \left(\frac{P}{\mu_0} x_2 + D_1 \right)^{\frac{1}{\alpha+1}} dx_2$$

which can be solved by using substitution method and we get

$$v_1(x_2) = 2^{\frac{\alpha}{2(\alpha+1)}} \frac{\mu_0(\alpha+1)}{P(\alpha+2)} \left(\frac{P}{\mu_0} x_2 + D_1 \right)^{\frac{\alpha+2}{\alpha+1}} + D_2 \tag{3.9}$$

where D_1 and D_2 are integration constants and will be specified later.

3.1.3 Application of the Boundary Conditions

To the integration constants, we need some boundary conditions. Let's consider the solutions after normalization and take no slip condition at the wall $v_1(x_2) = 0$ for $x_2 = 1$ and symmetry of the flow, which leads to the condition $\frac{\partial v_1}{\partial x_2}(x_2) = 0$ for $x_2 = 0$.

Applying these condition we get

$$v_1(x_2) = \frac{P}{2\mu}(x_2^2 - 1) \tag{3.10}$$

for the Newtonian fluid and

$$v_1(x_2) = -2^{\frac{\alpha}{2(\alpha+1)}} \frac{\alpha+1}{\alpha+2} \left(-\frac{P}{\mu_0} \right)^{\frac{1}{\alpha+1}} \left[x_2{}^{\frac{\alpha+2}{\alpha+1}} - 1 \right] \tag{3.11}$$

for the fluid approximated with power law model. Here we can see that the Newtonian model is only a special case of power-law model, if we consider $\alpha = 0$, we get the same models.

Still we need to go back to our assumptions we made while solving the power-law model. Applying the boundary conditions we get $D_1 = 0$, so considering $\frac{\partial v_1}{\partial x_2} < 0$ gives the solution for $x_2 > 0$, on the other hand considering $\frac{\partial v_1}{\partial x_2} > 0$ gives the same solution for $x_2 < 0$. And although we assumed $\frac{\partial v_1}{\partial x_2} \neq 0$, the one-sided limits as x_2 approaches to zero are the same and hence we can define $v_1(0)$ as value of this limit.

Now we will compare these two models for $P = -5$, $\alpha = -0.3$, $\mu = 3.5$.

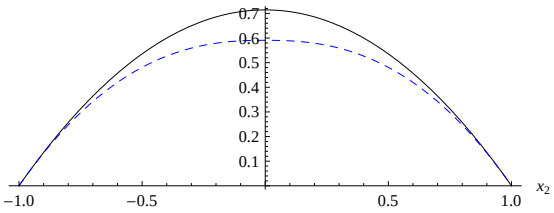


Figure 3.2: Comparison of constant model (3.10) (dashed) and power-law (full) viscosity model (3.11) for $P = -5$.

3.1.4 Different choice of constants

In the previous section we have been assuming $P = -5$. Let us have a look how the power-law model behaves for different values of pressure parameter P, viscosity μ and power-law coefficient α, see figures 3.3, 3.4 and 3.5.

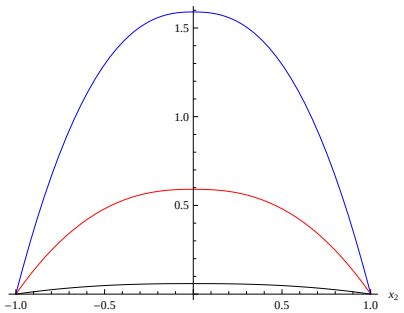


Figure 3.3: Comparison of power law model (3.11) for different values of pressure P. $P = 1$ (black), $P = 5$ (red), $P = 10$ (orange)

.

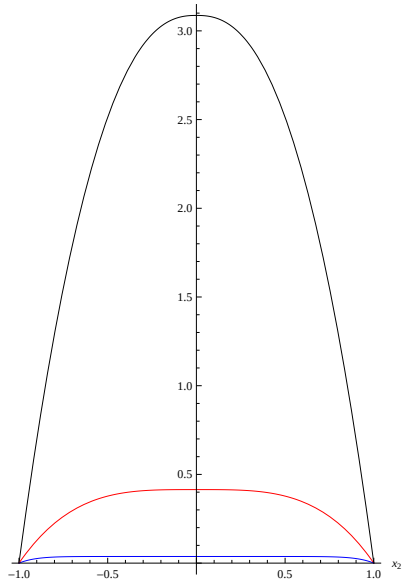


Figure 3.4: Comparison of power law model (3.11) for different values of viscosity μ. $\mu = 1.1$ (black), $\mu = 3.5$ (red), $\mu = 4$ (orange)

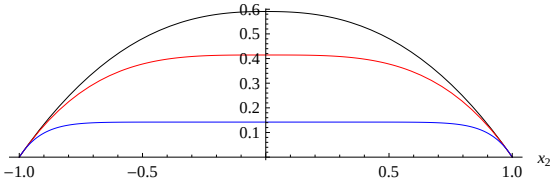


Figure 3.5: Comparison of power law model (3.11) for different values of power-law coefficient α. $\alpha = -0.3$ (black), $\alpha = -0.6$ (red), $\alpha = -0.9$ (orange)

3.1.5 Determination of pressure according to flow rate

As we are considering blood flow in a living organism, it could be difficult to measure pressure properly. Sometimes it is easier to measure the flow rate and specify the integration constants according to it. But mainly, comparing models for the same flow rate is the most appropriate comparison.

The flow rate in this context is defined by the following formula

$$Q(t) = \int_{-1}^{1} v(x,t)\,dx. \tag{3.12}$$

We will demonstrate this on the simplest Newtonian model. Computing flow rate using velocity that we get from equation (3.10) yields

$$Q(t) = -\frac{2}{3\mu}P. \tag{3.13}$$

Now we can use the knowledge of flow rate (we will assume $Q \equiv 1$) and get $P = -\frac{3\mu}{2}$. So the final form of the velocity is following

$$v_1(x_2) = -\frac{3}{4}(x_2^2 - 1) \tag{3.14}$$

Using the same method for Power-law model and assuming again $Q \equiv 1$ we get following solution

$$v_1(x_2) = -\frac{1}{2}\frac{2\alpha+3}{\alpha+2}\left(x_2^{\frac{\alpha+2}{\alpha+1}} - 1\right).$$

See figure 3.6 for comparison of these models.

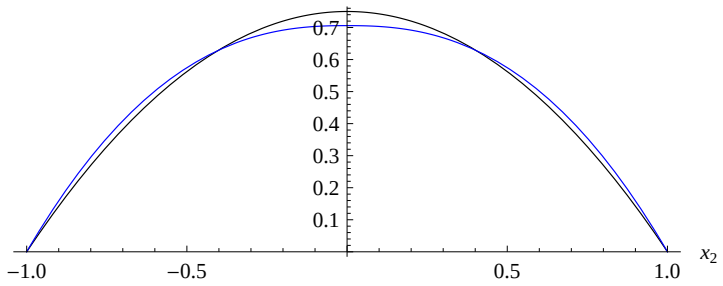


Figure 3.6: Comparison of Newtonian (black) and Power-law model (blue) for flow rate $Q \equiv 1$.

3.2 Two Fluid Models

Let's have a look on the Fahraeus-Lindquist effect now. It is assumed, that red blood cells are crowded near the tube center and close to the walls there are almost none of them as mentioned in the Introduction. This leads to a presumption, that there are different viscosities near the wall and in the central area of the tube, see [4]. The tube is split into two layers: the central area with radius r and viscosity μ_c and the outer layer with viscosity μ_0, see figure 3.7. The outer zone consists mostly of blood plasma, which has a similar behavior to water, so we will assume μ_0 being the viscosity of water.

Now we will try to approximate this with our two dimensional model of flow between two plates, see figure 3.8. Let us take two plates, and let us divide the area between them into three parts. The middle area will represent the middle of the vessel crowded with red blood cells. The zones near the plates (representing the vessel walls) will stand for the plasma layers.

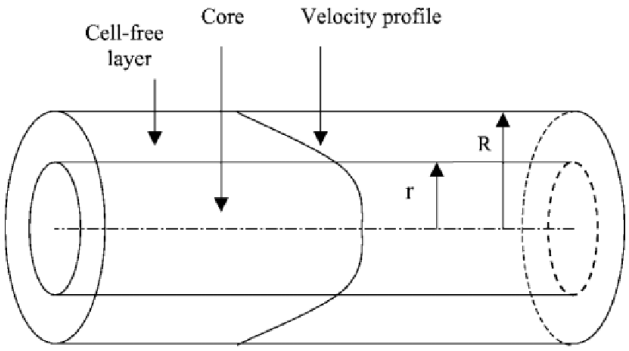


Figure 3.7: Two layer model, as mentioned in [5].

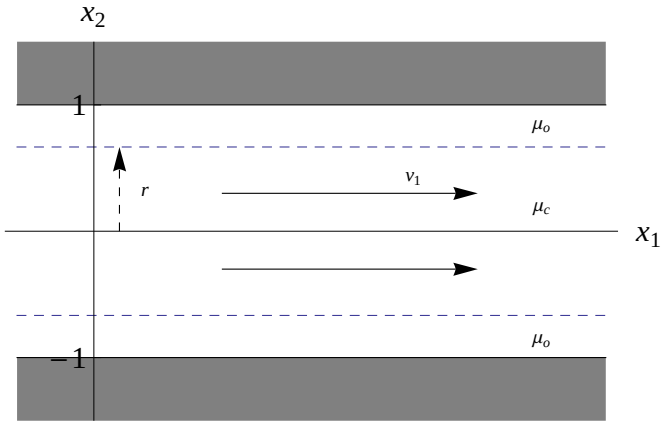


Figure 3.8: Two layer model in two dimensions.

3.2.1 Two fluid Constant Viscosity

Let v_0 be the velocity in the outer layer $|x_2| > r$ and v_c be the velocity in the inner layer $|x_2| \leq r$. Assuming constant viscosity, we solve the Navier-Stokes differential equations and get the solutions for the velocities in the two layers as

$$v_0(x_2) = \frac{P}{2\mu_0}x_2^2 + a_1x_2 + b_1, \quad r \leq x_2 \leq 1$$

$$v_c(x_2) = \frac{P}{2\mu_c}{x_2}^2 + a_2x_2 + b_2, \quad 0 \leq x_2 \leq r.$$

The two fluid flow is subject to following boundary and continuity conditions:
(a) no-slip condition

$$v_0(1) = 0,$$

(b) the continuity of velocity and shear stress at the layers' interface

$$v_0(r) = v_c(r),$$

$$\mu_c\frac{\partial v_c}{\partial x_2}|_{x_2=r} = \mu_0\frac{\partial v_0}{\partial x_2}|_{x_2=r}$$

(c) and the symmetry condition

$$\frac{\partial v_c}{\partial x_2}|_{x_2=0} = 0.$$

After application of previously stated boundary conditions (a) - (c) we get

$$v_0(x_2) = \frac{P}{2\mu_0}({x_2}^2 - 1), \quad r \leq x_2 \leq 1 \text{ and} \tag{3.15}$$

$$v_c(x_2) = \frac{P}{2\mu_0}\left[r^2 - 1 + \frac{\mu_0}{\mu_c}({x_2}^2 - r^2)\right], \quad 0 \leq x_2 \leq r. \tag{3.16}$$

3.2.2 Two fluid Power-law Model

Let's try the two layer model again, but now we will assume the power-law model for both of the viscosities μ_c and μ_o in the central, respectively outer zone, and we have

$$v_c(x_2) = 2^{\frac{\alpha}{2(\alpha+1)}}\frac{\mu_0(\alpha+1)}{P(\alpha+2)}\left(\frac{P}{\mu_0}\,x_2 + D_1\right)^{\frac{\alpha+2}{\alpha+1}} + D_2, \quad 0 \leq x_2 \leq r. \tag{3.17}$$

and

$$v_0(x_2) = 2^{\frac{\beta}{2(\beta+1)}}\frac{\mu_0(\beta+1)}{P(\beta+2)}\left(\frac{P}{\mu_0}\,x_2 + C_1\right)^{\frac{\beta+2}{\beta+1}} + C_2, \quad r \leq x_2 \leq 1. \tag{3.18}$$

where

$$\mu_c = \mu\,|\mathbb{D}|^{\alpha}$$

and

$$\mu_0 = \mu\,|\mathbb{D}|^{\beta}\,.$$

When we consider the boundary conditions (a) - (c) stated above, we get an analytical solution shown, which is quite complicated so we only show the resulting figure, see 3.9

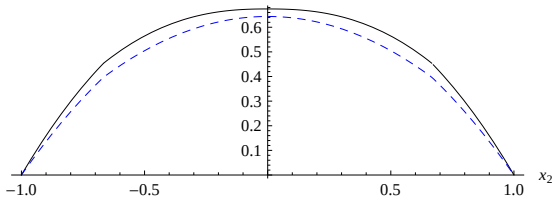


Figure 3.9: Comparison of two fluid constant (dashed) and power-law (full) viscosity models.

3.2.3 Two fluid combined Model

As we know that plasma has similar properties to water, which is a Newtonian fluid, it looks like we could approximate the almost particle-free outer layer with the constant viscosity model and use the power-law model for the central area filled with particles.

Let us consider $\mu_c = \mu\left(\epsilon + |\mathbb{D}|^2\right)^{\frac{\alpha}{2}}$ as the viscosity in central area of the tube, but as we assume $\epsilon = 0$, this can be further simplified to $\mu_c = \frac{\mu}{2}\left|\frac{\partial v_c}{\partial x_2}\right|^{\alpha}$. Then we assume velocity in following form

$$v_0(x_2) = \frac{P}{2\mu}x_2^2 + C_1 x_2 + C_2, \quad r \leq x_2 \leq 1 \tag{3.19}$$

where μ_0 is the constant viscosity and

$$v_c(x_2) = 2^{\frac{\alpha}{2(\alpha+1)}}\frac{\mu(\alpha+1)}{P(\alpha+2)}\left(\frac{P}{\mu}\,x_2 + D_1\right)^{\frac{\alpha+2}{\alpha+1}} + D_2, \quad 0 \leq x_2 \leq r. \tag{3.20}$$

According to boundary conditions (a) - (c) on page 14 we are able to specify the integration constants C_1, C_2, D_1 and D_2 and get the solution

$$v_0(x_2) = (x_2 - 1)\left(\frac{P}{2\mu_0}(x_2+1) - \frac{P}{\mu_0}r + \left(2^{\frac{\alpha}{2}}\frac{Pr}{\mu_0}\right)^{\frac{1}{\alpha+1}}\right) \tag{3.21}$$

and

$$v_c(x_2) = 2^{\frac{\alpha}{2(\alpha+1)}}\frac{\mu_0(\alpha+1)}{P(\alpha+2)}\left(\frac{P}{\mu_0}x_2\right)^{\frac{\alpha+2}{\alpha+1}} + D_2 \tag{3.22}$$

where $D_2 = -\frac{P}{2\mu_0}(r-1)^2 + \left(2^{\frac{\alpha}{2}}\frac{P}{\mu_0}r\right)^{\frac{1}{\alpha+1}}\left(\frac{r}{\alpha+2} - 1\right)$. See the solution on figure 3.10.

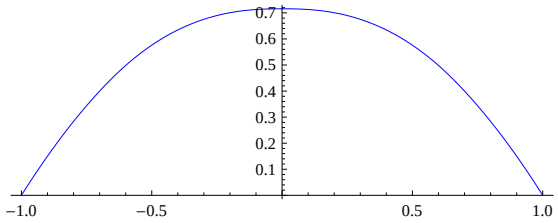


Figure 3.10: Visualization of combined model: outer layer with constant viscosity, core layer with power-law viscosity model. (Scaled for flow rate $Q \equiv 1$)

3.2.4 Comparison of the models

Figure 3.11 shows, that each of the models gives slightly different velocity profile, but if we compare them for the same flow rate, some similarities can be found. The velocity gradient jump at position $r = \frac{2}{3}$ might be explained with the viscosity change while the pressure remains the same. Also, we were assuming that r remains the same while viscosity is changing, but according to the experiments in [4] the r is changing with changing velocity and viscosity. Moreover, we are only considering an x_2 independent pressure which does not give much possibility to smooth out this jump.

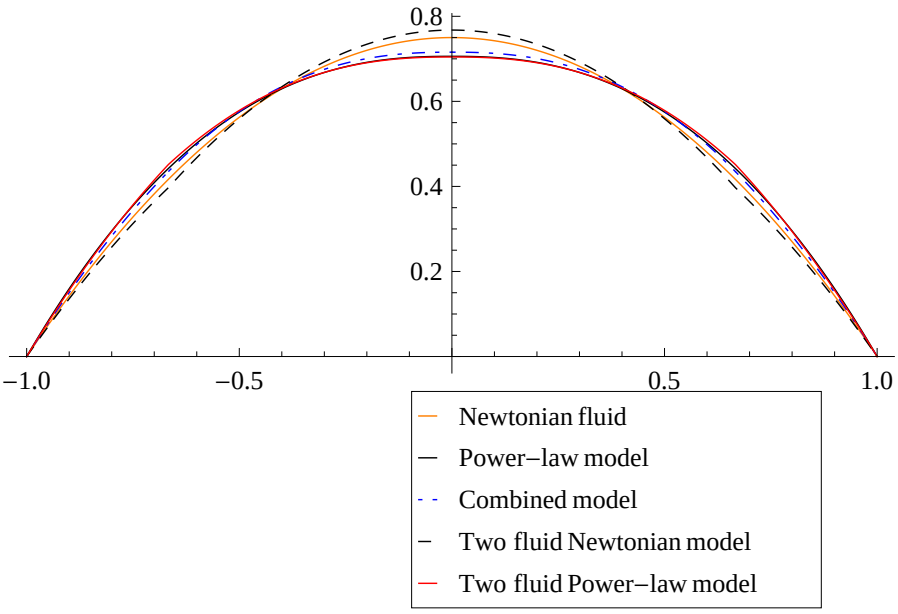


Figure 3.11: Comparison of all the models mentioned in this section

4. Pulsatile Flow

Considering pulsatile blood flow is the next step to improving our model. We will keep on working with the Poisseuille flow assumptions where $\boldsymbol{v}(t, x_1, x_2) = (v_1(t, x_2), 0)$.

4.1 Derivation of the basic equation

The pulsation can be approximated by periodically changing pressure gradient. Let us assume $\frac{\partial \tilde{p}}{\partial x_1} = P\cos(\omega t)$, where ω is the frequency and P is the amplitude of the pressure oscilation. Rewriting the momentum equations using mentioned simplifications and the fact that viscosity μ is constant yields

$$\frac{\partial v_1}{\partial t} - \frac{\mu}{\rho}\frac{\partial^2 v_1}{\partial x_2^2} = -P\cos(\omega t), \tag{4.1}$$

which is a partial differential equation of second order, so called parabolic type equation.

4.2 Analytical solution for oscillating pressure

To solve equation (4.1) analytically, we need to assume constant viscosity, so we will show this analytically for the single fluid Newtonian model.

Let us consider following form of pressure gradient $\frac{\partial \tilde{p}}{\partial x_1} = Pe^{i\omega t}$. We will find the complex solution[1] at first and then we will consider the real part of this solution. According to [2] we can now assume the solution in following form: $\tilde{v_1}(t, x_2) = V(x_2)\, e^{i\omega t}$, where we separate the space and time variables into different functions. On substituting this into equation (4.1) we get

$$i\omega V(x_2)\, e^{i\omega t} - \frac{\mu}{\rho}V''(x_2)\, e^{i\omega t} = Pe^{i\omega t}$$

which can be simplified to

$$V''(x_2) - \frac{i\omega\rho}{\mu}V(x_2) = -\frac{P\rho}{\mu}.$$

This is a linear ordinary differential equation for unknown $V(x_2)$ and the standard solution is

$$V(x_2) = C_1 e^{iBx_2} + C_2 e^{-iBx_2} - \frac{iP}{\omega},$$

where $B = \sqrt{\frac{i\omega\rho}{\mu}}$. Now the complex velocity is

$$\tilde{v_1}(t, x_2) = e^{i\omega t}\left[C_1 e^{iBx_2} + C_2 e^{-iBx_2} - \frac{iP}{\omega}\right]. \tag{4.2}$$

and we only need to separate its real part.

[1] For distinguishing real and complex functions, we will use the tilde; $\tilde{p}$ is the complex pressure and p is the real pressure.

Using the identity

$$e^{iBx_2} = e^{-x_2 H}\left(\cos x_2 H + i \sin x_2 H\right)$$

with $H = \frac{B}{\sqrt{2i}} = \sqrt{\frac{\omega\rho}{2\mu}}$ and $C_1 = a_1 + ib_1$, $C_2 = a_2 + ib_2$ we can separate the real and imaginary part of the complex velocity (4.2). Applying the boundary conditions on the real part $v_1(t,1) = v_1(t,-1) = 0$ we get four linear equations for a_1, a_2, b_1 and b_2

$$\begin{aligned}
0 &= \frac{P}{\omega} - \cos H(b_1 e^{-H} + b_2 e^{H}) + \sin H(a_2 e^{H} - a_1 e^{-H}) \\
0 &= \cos H(a_1 e^{-H} + a_2 e^{H}) + \sin H(b_2 e^{H} - b_1 e^{-H}) \\
0 &= \frac{P}{\omega} - \cos H(b_1 e^{H} + b_2 e^{-H}) - \sin H(a_2 e^{-H} - a_1 e^{H}) \\
0 &= \cos H(a_1 e^{H} + a_2 e^{-H}) - \sin H(b_2 e^{-H} - b_1 e^{H}).
\end{aligned}$$

Solving these linear equations yields

$$a_1 = a_2 = a = \frac{P e^{H}\left(1 - e^{2H}\right)\sin H}{\omega\left(\cos^2 H\left(e^{2H}+1\right)^2 + \sin^2 H\left(e^{2H}-1\right)^2\right)}$$

$$b_1 = b_2 = b = \frac{P\cos H\left(1 - e^{2H}\right)}{\omega\left(\cos^2 H\left(e^{2H}+1\right)^2 + \sin^2 H\left(e^{2H}-1\right)^2\right)}$$

On substituting these constants into the real part of (4.2) we get the final solution

$$\begin{aligned}
v_1(t, x_2) = {} & 2\cos x_2 H \cosh x_2 H\left(a\cos\omega t - b\sin\omega t\right) + \frac{P}{\omega} \\
& + 2\sin x_2 H \sinh x_2 H\left(a\sin\omega t + b\cos\omega t\right).
\end{aligned} \tag{4.3}$$

On figures (4.1), (4.2) and (4.3) we can see how the solution behaves for different t. In this visualization we used constants $P = 5$, $\mu = 3.5$ and $\omega = 2\pi$.

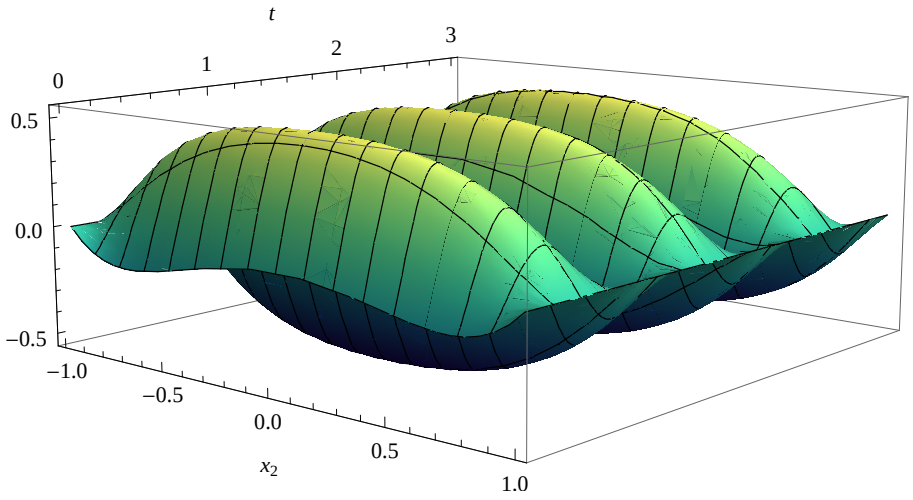


Figure 4.1: Newtonian model for pulsatile flow: visualization of analytical solution for time $t = 0...3$.

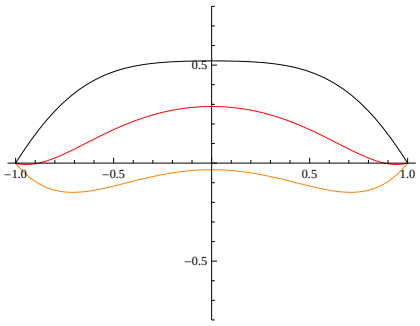


Figure 4.2: Newtonian model for pulsatile flow: Velocity profiles for $t = 0$ (orange), $t = 0.1$ (red) and $t = 0.3$(black).

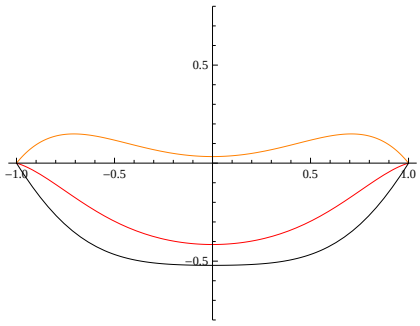


Figure 4.3: Newtonian model for pulsatile flow: Velocity profiles for $t = 0.5$ (orange), $t = 0.65$ (red) and $t = 0.8$(black).

4.3 Numerical solution for oscillating pressure

In this section we will show numerical results which we got using Mathematica's function NDSolve which uses combination of method of lines for discretization in time and finite difference method for discretization in space. We got our results using Wolfram Mathematica, see the full code in Attachments on page 28.

For comparison of the models we will use following values of constants: $P = 5$, $\mu = 3.5$, $\omega = 2\pi$ and $\alpha = -0.3$.

4.3.1 One-fluid models

We will start with the power-law model ($\alpha = -0.3$), see figures 4.4, 4.5 and 4.6.

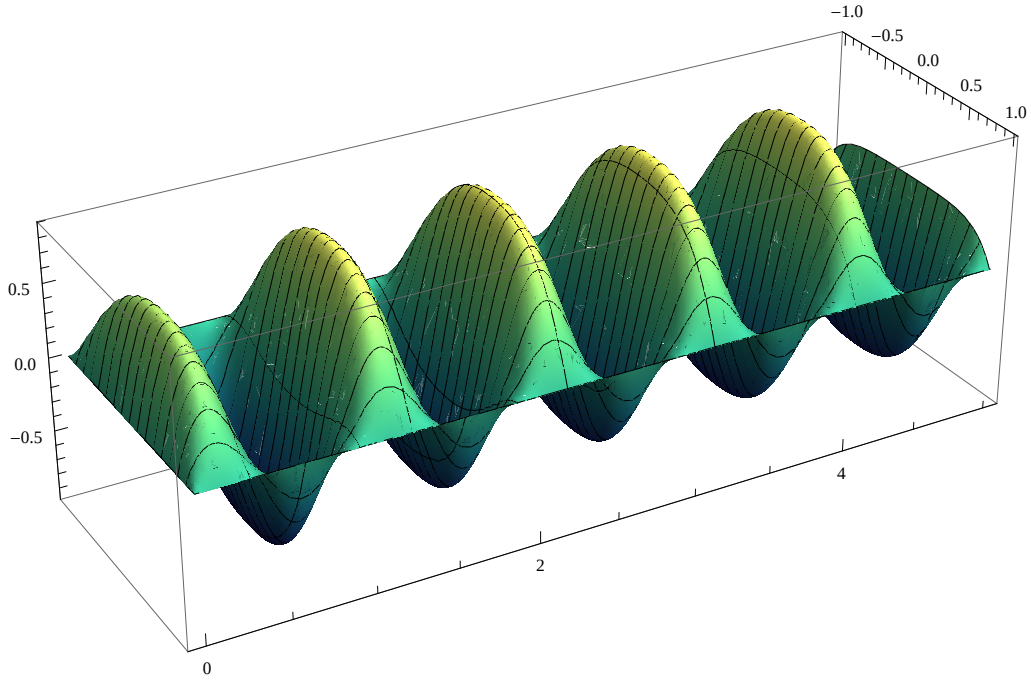


Figure 4.4: One fluid power-law model: Visualization of velocity profiles for time $t = 0...5$.

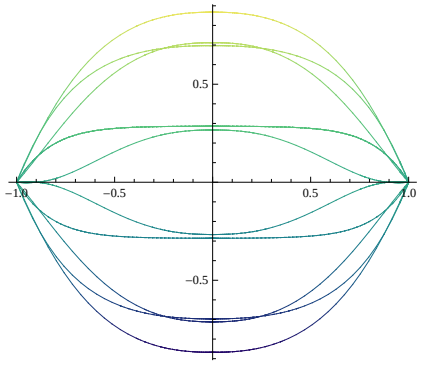


Figure 4.5: One fluid power-law model: Velocity profiles for $t = 9..10$.

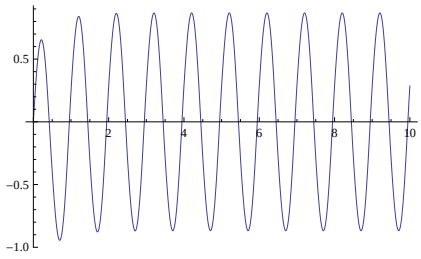


Figure 4.6: One fluid power-law model: Visualization of velocity profile for $x_2 = 0$.

It is interesting, what happens as α approaches to -1. See figures 4.7, 4.8 and 4.9 to see the difference for $\alpha = -0.9$. For comparison with models for $\alpha = -0.3$ see figures 4.4, 4.5 and 4.6.

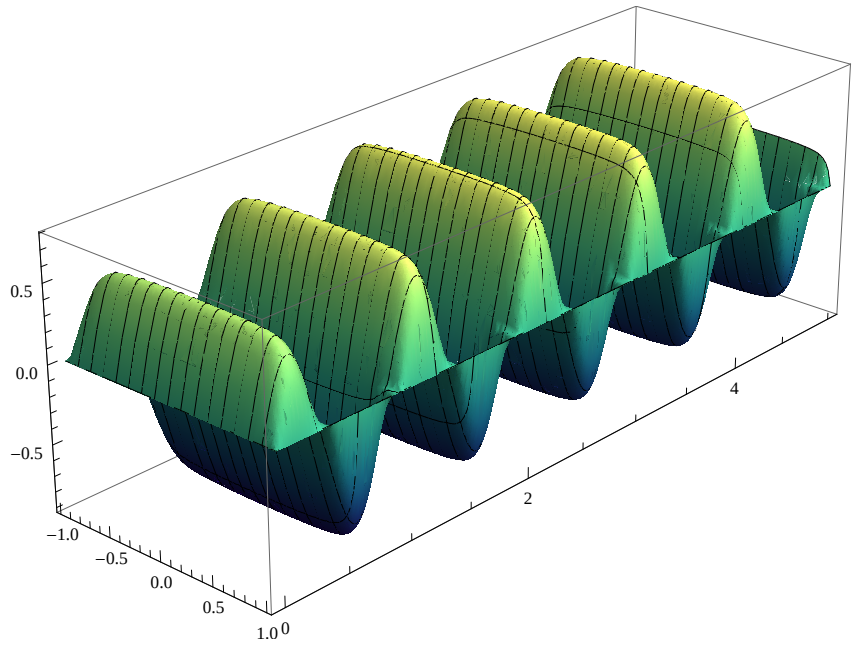


Figure 4.7: One fluid power-law model: Visualization of velocity profiles for time $t = 0...5$ and $\alpha = -0.9$.

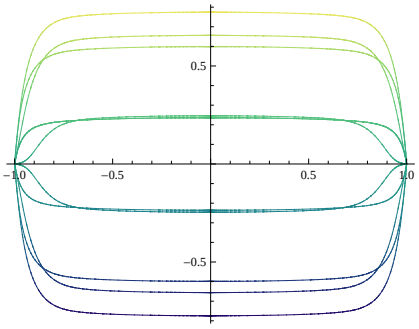


Figure 4.8: One fluid power-law model: Velocity profiles for $t = 9..10$ and $\alpha = -0.9$.

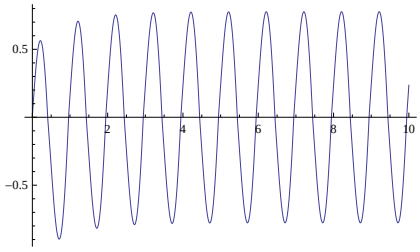


Figure 4.9: One fluid power-law model: Visualization of velocity profile for $x_2 = 0$ and $\alpha = -0.9$.

4.3.2 Two-fluid models

Now let us discuss the two fluid models. On figures 4.10, 4.11 and 4.12 we can see, how the fluid's velocity behaves if we approximate both layers with Newtonian model. We used following values: $\mu_0 = 1.1$ as the plasma viscosity in the outer layer and $\mu_c = 3.5$ for the inner layer viscosity.

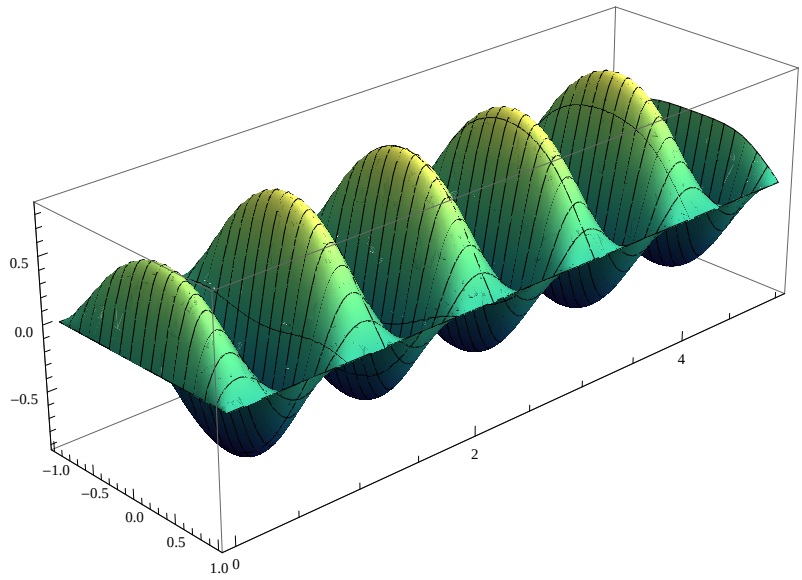


Figure 4.10: Two fluid Newtonian model: Visualization of velocity profile for time $t = 0...5$.

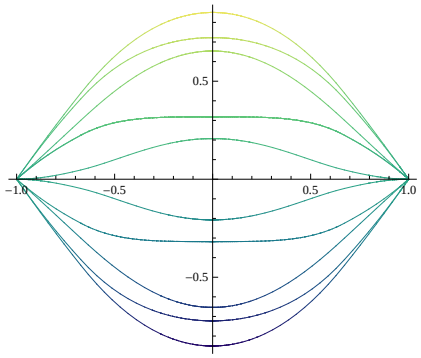


Figure 4.11: Two fluid Newtonian model: Velocity profiles for $t = 9..10$.

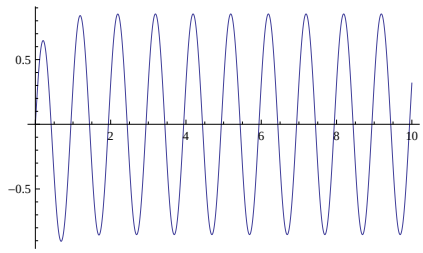


Figure 4.12: Two fluid Newtonian model: Visualization of velocity profile for $x_2 = 0$.

The one of our models which is closest to reality is probably the combined two fluid model. Here we assume the central area to be a power-law fluid with $\alpha = -0.3$ and assume plasma at the walls to behave like a Newtonian fluid with $\mu = 1.1$. See figures 4.13, 4.14 and 4.15.

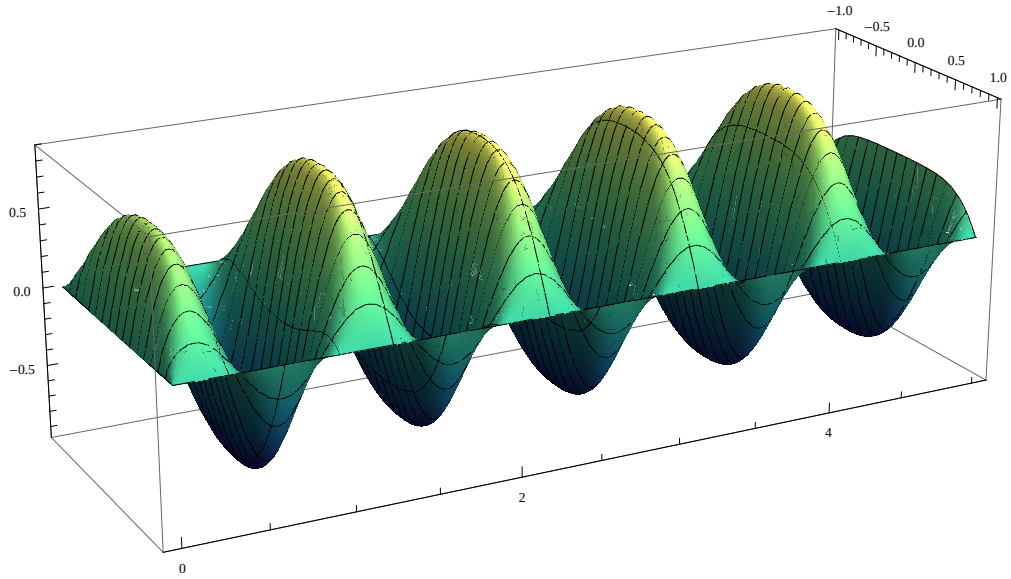


Figure 4.13: Combined model: Visualization of velocity profile for time $t = 0...3$.

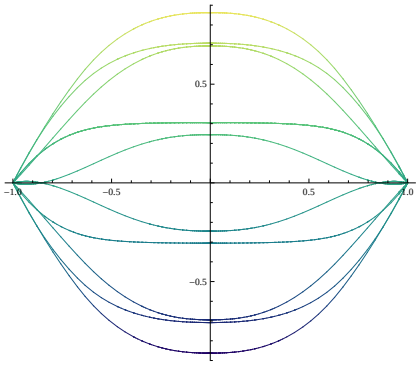


Figure 4.14: Combined model: Velocity profiles for $t = 9..10..$

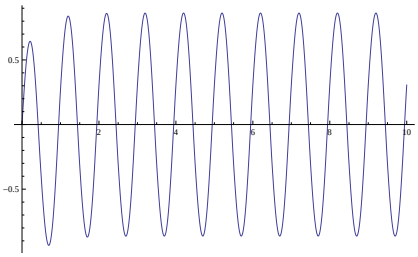


Figure 4.15: Combined model: Visualization of combined model for velocity profile for $x_2 = 0$.

4.4 Numerical solution for shifted pressure

To get closer the the properties of real physiological blood flow we consider pressure gradient of the form $\frac{\partial p}{\partial x_1} = P\left(\cos\left(\omega t\right) + 1\right)$. See figures 4.16, 4.17 and 4.18 for the resulting numerical solution. For visualization we used again following constants $P = 5$, $\mu = 3.5$ and $\omega = 2\pi$.

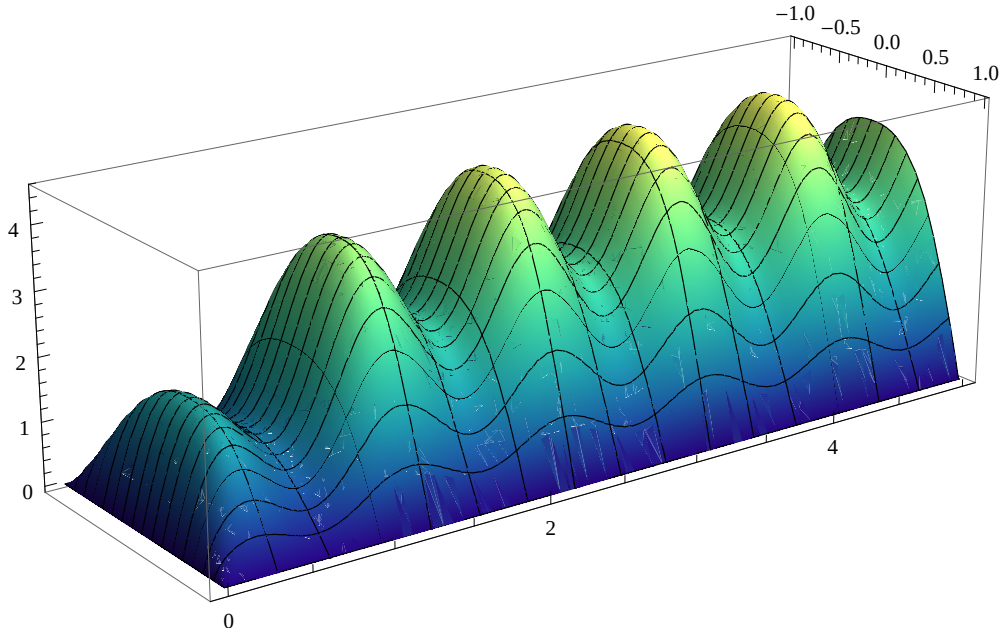


Figure 4.16: Increased pressure gradient model: Visualization of velocity profile for time $t = 0...3$.

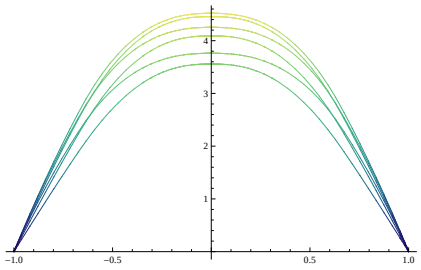


Figure 4.17: Increased pressure gradient model: Velocity profiles for $t = 9..10..$

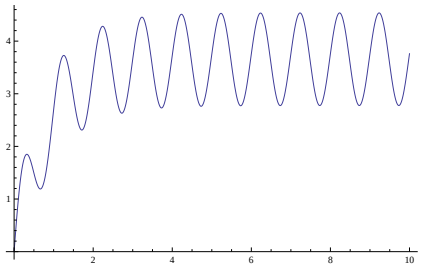


Figure 4.18: Increased pressure gradient model: Visualization of combined model for velocity profile for $x_2 = 0$.

Epilogue

In chapter 3 we show velocity profiles for steady Poisseuille flow. Through the whole work we use two basic models for viscosity: the Newtonian model with constant viscosity and Power-law model where the viscosity changes with shear rate.

According to measurements and observations carried out by [4] we try to model the Fahraeus-Lidquist effect. The main attribute of this effect is a higher concentration of blood particles in the central area of the vessel and therefore we use two-fluid approximation where we use different models of viscosity for each layer.

In chapter 4 we extend our models to pulsatile flow. Most of the models were solved numerically using Mathematica, only one-layer Newtonian model was solved analytically. Our best model is the combined model on page 24 which approximates the plasma as a Newtonian fluid and the central layer as power-law fluid.

At the end of our work we solve the pulsatile flow with shifted pressure gradient which is probably the closest to the reality. In the previous models we were assuming that pressure gradient gets also to negative values, which is eliminated when we consider the shifted gradient. We would get better result if we approximated the actual physiological pressure pulse with Fourier series.

For even better approximation we need to use a 3D model with cylindrical coordinates instead of our two dimensional simplification. The next step could be shear rate or velocity dependent position of the border between the two layers used in the two-fluid models.

Bibliography

[1] Fung, Y.C. *Biomechanics: Mechanical Properties of Living Tissues*. 2nd ed. Springer New York, 1993. ISBN 0-387-97947-6.

[2] Mazumdar, J. *An Introduction to Mathematical Physiology and Biology*. 2nd ed. Cambridge University Press, 1999. ISBN 9780521646758.

[3] Ganong, W.F. *Přehled lékařské fyziologie*. H&H, 1995. ISBN 9788085787368.

[4] Aarts, P.A., van den Broek, S.A., Prins, G.W., Kuiken, G.D., Sixma, J.J., Heethaar, R.M. *Blood platelets are concentrated near the wall and red blood cells, in the center in flowing blood*. Arteriosclerosis, Thrombosis, and Vascular Biology, 1988. ISSN 1079-5642.

[5] Sharan, M., Popel, A.S. *A Two-Phase Model for Flow of Blood in Narrow Tubes With Increased Effective Viscosity Near the Wall*. IOS Press, 2001. ISSN 415–428.

[6] Zaeem, M.A., Lapin, S., Matveev, K. *The Effect of Vibration on Flow Rate of Non-Newtonian Fluid*. SIAM, 2009. ISBN 978-0-898719-34-5.

[7] Valenta, J. *Biomechanics*. 2nd ed. Elsevier, 1993. ISBN 9780444987648.

[8] Marcinkowska-Gapinska, A., Gapinski, J., Elikowski, W., Jaroszyk, F., Kubisz, L. *Comparison of three rheological models of shear flow behavior studied on blood samples from post-infarction patients*. Springer, 2007. ISSN 837-844.

[9] `www.wikipedia.com`

Attachments

The input for Mathematica we used to get numerical results for pulsatile flow in chapter 4.

```
(* equation *)
eq = { D[v[x, t], t] ==
    D[    \[Mu][x, D[v[x, t], x]] * D[v[x, t], x]    , x] +
     P* Cos[\[Omega] t]} ;

(* boundary and initial conditions *)
bc = {v[x, 0] == 0, v[-1, t] == 0, v[1, t] == 0};

sol = NDSolve[
 {eq, bc}, v, {x, -1, 1}, {t, 0, 10},
 MaxStepSize -> 0.01, AccuracyGoal -> 6,
 PrecisionGoal -> 6, MaxSteps -> 10^6,
 Method -> {"MethodOfLines",
 "SpatialDiscretization" ->
 {"TensorProductGrid",
   "MaxStepSize" -> 0.01,
   "AccuracyGoal" -> 0,
   "PrecisionGoal" -> 0,
   "DifferenceOrder" -> 2}}
]

Plot3D[Evaluate[First[v[x, t] /. sol]], {x, -1, 1}, {t, 0, 5},
 PlotPoints -> {20, 80}, PlotRange -> All, BoxRatios -> {1, 3, 1},
 ColorFunction -> "BlueGreenYellow"]
```